

Capped carbon nanotubes with a number of ground state magnetization discontinuities increasing with their size

N. P. Konstantinidis

Leoforos Syggrou 360, Kallithea 17674, Athens, Hellas

(Dated: December 15, 2015)

The classical ground state magnetic response of fullerene molecules that resemble capped carbon nanotubes is considered within the framework of the antiferromagnetic Heisenberg model. It is found that the magnetic response depends subtly on spatial symmetry, similarly to the strong dependence of the conductive properties of carbon nanotubes on their chirality. Clusters based on armchair carbon nanotubes which are capped with non-neighboring pentagons and have D_{5d} spatial symmetry have a number of magnetization discontinuities which increases with their size. This occurs even though the model completely lacks magnetic anisotropy, and even though the only source of frustration are the two groups of six pentagons located at the ends of the molecules, which become more strongly outnumbered as the clusters are filled in the middle with more unfrustrated hexagons with increasing size. For the cluster with 180 vertices there are already seven magnetization and one susceptibility discontinuities. Contrary to that, similar molecules with D_{5h} spatial symmetry reach a limit of one magnetization and two susceptibility ground state discontinuities, while the corresponding clusters capped by neighboring pentagons also reach a fixed number of discontinuities with increasing size.

PACS numbers: 61.48.De Carbon Nanotubes, 75.10.Hk Classical Spin Models, 75.50.Ee Antiferromagnetics, 75.50.Xx Molecular Magnets

Carbon nanotubes are cylindrically structured allotropes of carbon that form aesthetically pleasing hexagonal shapes, with each carbon atom covalently bonded to other three [1–5]. Their topology is the one of the fullerene family, and they are formed by graphene sheets rolled at specific angles. They possess a large number of unusual mechanical, electrical and thermal properties. Their diameter can be as small as 1 nm and their length as big as several centimeters, bridging the molecular and macroscopic scales. The ends of the nanotubes can be closed by carbon atoms that form pentagons at the ends of the nanotube [6]. They are very strong with a strength that can be over ten times that of any industrial fiber [7], while their conducting properties are strongly dependent on the chirality and diameter of the hexagonal lattice along the nanotube. Armchair carbon nanotubes are metallic and can support very high currents, while zigzag and chiral carbon nanotubes are semiconducting [8–11]. The thermal conductivity of carbon nanotubes at room temperature can exceed the thermal conductivity of diamond [12]. Commercial production of carbon nanotubes has surged during the last decade, and they are used in such diverse products as batteries, boat hulls, thin-film electronics and vehicle parts.

From the theoretical point of view, the electronic properties of the nanotubes are closely connected to the ones of graphene [13, 14]. Their low-dimensionality qualifies them as a good testing ground for strongly correlated interactions [15, 16]. Due to experimental difficulties electron correlations effects have been difficult to observe, and a tight-binding picture has been adopted. However experiments with very clean samples highlighted the importance of electron correlations [17–21]. In this paper we consider carbon nanotubes capped at their edges with

carbon atoms that form pentagons, thereby having the shape of fullerene molecules. We consider electrons residing at the vertices of the nanotubes that interact according to the antiferromagnetic Heisenberg model (AHM), which is derived from the Hubbard model at half-filling with very strong on-site electron interaction U [22, 23]. We find that when the spins are classical the magnetization response in a field has a number of magnetization discontinuities which increases with the size of the capped nanotube when the pentagons at the edges do not neighbor each other. These discontinuities are as many as seven already for the molecule with 180 vertices. This is unexpected for a model lacking magnetic anisotropy, and shows that the nanotubes under consideration can be used as relatively small magnetic entities where the magnetization can be tuned between many different regimes with application of a magnetic field. For slightly different symmetry or caps the number of magnetization and susceptibility discontinuities does not eventually change with the size of the nanotube, showing that the magnetic response depends subtly on symmetry and the specific topology of the cap.

Single-wall carbon nanotubes are ideal one-dimensional mesoscopic systems and can behave as quantum waveguides [24] and quantum dots [25–27]. Oxygen molecules encapsulated in single-wall carbon nanotubes form a one-dimensional $s = 1$ Haldane magnet [28]. Lattices and clusters of frustrated topology are of special interest, as they are associated with unexpected magnetic behavior [29–31]. Fullerenes are carbon structures that come among others in the form of hollow spheres (molecules) or nanotubes [32]. Fullerene molecules consist of 12 pentagons and $\frac{N}{2} - 10$ hexagons which share edges, with N the number of the molecule's

vertices, which are three-fold coordinated. Frustration is introduced by the the pentagons, and consequently decreases on the average with N . C_{60} , which has the shape of a truncated icosahedron and belongs to the icosahedral symmetry group I_h [33], superconducts when doped with alkali metals [34], and belongs to the intermediate U regime of the Hubbard model [35, 36]. For the AHM the magnetization response of the I_h fullerenes is discontinuous at the classical and quantum level [37–39]. This is not expected for a model lacking magnetic anisotropy. For relatively small fullerene molecules of other symmetries there are only pronounced magnetization plateaus for $s = 1/2$ [40]. Furthermore the icosahedron, not a fullerene but the smallest cluster with I_h symmetry, has a classical ground state magnetization discontinuity which persists for lower values of s [41, 42]. It is also noted that in numerical calculations U has been found to be stronger for C_{20} than C_{60} [43, 44], further supporting the validity of the AHM as a good description of the Hubbard model for the I_h fullerenes. The above results show strong correlations between spatial symmetry and magnetic response for a fullerene molecule, which have also been demonstrated for the dodecahedron and the icosahedron [38].

Motivated by the subtle dependence of the conductive properties of carbon nanotubes on their topology, and by the magnetization discontinuities of the aforementioned fullerene molecules, we undertake in this paper the question of the magnetic response of fullerene molecules that resemble capped carbon nanotubes. They have the cylindrical structure of armchair nanotubes, and on each end they are capped by a group of six pentagons, with the pentagons not neighboring each other (Fig. 1(a)) [45]. These structures provide a link between molecular fullerenes and carbon nanotubes, being capped versions of (5,5) single-walled carbon nanotubes. The smallest member of the class is C_{60} , while bigger molecules have either a number of vertices which is an even multiple of 10 and D_{5d} spatial symmetry, or a number of vertices which is an odd multiple of 10 and D_{5h} spatial symmetry. Ideal graphene is nonmagnetic, but many of its derivatives are. The nearest-neighbor tight-binding model, which corresponds to the hopping term of the Hubbard model, has been shown to describe accurately the electronic structure of graphene and derivatives of it [46]. To introduce magnetism the on-site Coulomb interaction is added in the Hubbard model. Here we consider its large U limit at half-filling, the AHM, which is expected to be relevant for the physical case of intermediate U [37]. We do so in order to examine correlations between spatial symmetry and the number of ground state magnetization and susceptibility discontinuities in a field, when classical spins are mounted on the molecule vertices. Frustration originates in the two pentagon subblocks that cap the edges. We find that the D_{5d} molecules have a number of ground state discontinuities which increases with their size, and goes up to seven magnetization and one susceptibility

jumps for the largest cluster considered, which has 180 vertices. This number far supersedes the three magnetization gaps of the dodecahedron, and indicates that the total number of ground state discontinuities is controlled by the size of the molecule and will keep increasing for bigger members of this class. For the D_{5h} symmetry clusters the number of discontinuities remains three for the largest calculated sizes, with one magnetization and two susceptibility discontinuities. This shows that fine differences in the topology can have a significant effect on the magnetic properties of the nanotube-like molecules, similar to the effects detected in their electronic structure properties [8–11]. This conclusion is further supported by fullerene molecules that have a carbon nanotube shape and are capped at their edges with neighboring pentagons, and have a total number of discontinuities that is size independent.

The Hamiltonian of the AHM is

$$H = J \sum_{\langle ij \rangle} \vec{s}_i \cdot \vec{s}_j - h \sum_{i=1}^N s_i^z \quad (1)$$

J is the exchange interaction strength, taken to be 1 from now on. $\langle ij \rangle$ indicates that interactions are limited to nearest neighbors. The magnetic field \vec{h} is taken along the \hat{z} axis, and the spins are classical vectors with unit magnitude. In Hamiltonian (1) the exchange competes with the magnetic energy, with the frustrated connectivity playing an important role. Minimization of the Hamiltonian gives the ground state energy and spin configuration for any magnetic field [37–39, 42, 47, 48].

The importance of frustration is seen in the lowest energy configuration magnetic response of the group of six pentagons located at the ends of the molecules, when it is completely isolated (Fig. 1(a)). Pentagons introduce frustration in fullerene molecules, since an isolated pentagon can not have all antiferromagnetically interacting nearest-neighbor spin pairs simultaneously pointing in opposite directions, due to the odd number of spins and the closed periodic boundary conditions. In contrast, this is possible for an isolated hexagon. The magnetization curve of the six-pentagon subblock provides an insight on the properties of the whole cluster, as it is the sole carrier of frustration. Nearest neighbor intrapentagon interactions are taken equal to J and interpentagon interactions equal to J' (Fig. 1(a)). The ground state magnetization and susceptibility discontinuities are shown in Fig. 1(b) as functions of $\frac{J'}{J}$ and h . When $J' = 0$ the magnetization curve corresponds to that of an isolated pentagon, which has constant susceptibility up to saturation. A non-zero J' does not introduce further frustration as it does not change the energy of any of the six pentagons in zero field, with neighboring spins belonging to different pentagons antiparallel. However the interpentagon coupling generates two ground state magnetization gaps in a field, which survive up to $J' = J$ (App. A). The lowest field magnetization discontinuity is flanked by susceptibility discontinuities, which disappear for higher J' .

The molecules considered in this paper are formed by filling the space between two such six-pentagon subblocks with an armchair carbon nanotube structure, which is solely made up of hexagons. When the pentagons and the nanotube structure are brought together to form the cluster further frustration is introduced, as the lowest energy is slightly higher than the sum of the energies of the isolated pentagons and hexagons (App. B). Furthermore we find that the ground state magnetization curve of the fullerene molecules under consideration has more discontinuities than those of the isolated six-pentagon subblocks, and the number of these discontinuities increases with N . The smallest member of the class is the truncated icosahedron for which $N = 60$, which is already known to possess two magnetization jumps [39]. The smallest member of the class with D_{5d} symmetry has $N = 80$ and five discontinuities in total. Fig. 2 shows how these discontinuities evolve from the isolated six-pentagon subblock limit when 20 spins are introduced in the middle to form the cluster. When the three parts that form the molecule are not interacting ($J_1 = 0$) there are two magnetization discontinuities due to the pentagon subblocks according to Fig. 1(b), as well as a susceptibility discontinuity originating in the saturation field of the nanotube part. This equals 4, which is the saturation field of an isolated hexagon. Increasing the coupling J_1 between the nanotube and the pentagon subblocks results in a rather complicated discontinuity diagram plotted as a function of J_1 and the magnetic field h , with many magnetization and susceptibility discontinuities. The low-field susceptibility and magnetization jumps at the uniform interaction limit $J_1 = 1$ are traced back to the low-field magnetization discontinuity of the pentagon subblocks. On the other hand, the high-field discontinuities at $J_1 = 1$ trace themselves back to all the discontinuities present when $J_1 = 0$. For the icosahedron it has been shown that its classical magnetization gap originates in the magnetization discontinuity of two isolated spins that connect with a triangular strip to form the icosahedron [42]. Figure 2 shows that similar considerations for the $N = 80$ cluster lead to more complicated results, as the parts that make it up are more complex in comparison with the icosahedron.

Figures 3(a) and 3(b) show respectively the location of the low- and high-field ground state magnetization and susceptibility discontinuities for the D_{5d} molecules as functions of N and the reduced magnetic field $\frac{h}{h_{sat}}$, with h_{sat} the saturation magnetic field. For both low and high fields the number of magnetization jumps increases with N . Initially there is only one low-field magnetization gap for $N = 60$, and by $N = 180$ there are already four. For high fields the corresponding numbers are one for $N = 60$ and three for $N = 180$, to which a susceptibility discontinuity is added. Figure 3(a) hints to the fact that new ground state discontinuities emerge close to the highest low-field discontinuity, as can be seen for $N = 120$ and 160. The discontinuities move away from each other with increasing N . Similarly for the high-field jumps in Fig.

3(b), new ones emerge for $N = 80$ and 140, but now the discontinuities approach each other with increasing N . The low-field susceptibility discontinuity gives way to a magnetization discontinuity for higher N , while the high-field susceptibility jump persists up to $N = 180$. Another feature of the jumps at least for high fields is that they tend to constant values of $\frac{h}{h_{sat}}$ with N . The corresponding changes in the magnetization per spin are shown in Fig. 3(e). The low-field ground state discontinuities are associated with a stronger magnetization change, which is as big as $\Delta M = 0.760$ for $N = 180$.

Specific features of the discontinuities can be detected (App. C). For low fields as well as just before saturation some of the pentagon spins are parallel or antiparallel with the magnetic field, and their deviation from or alignment with these directions generates respectively the lowest and highest field discontinuities. The last low-field magnetization discontinuity, which is associated with the strongest magnetization change, occurs as pentagon spins change from having the lowest to having the highest total magnetizations along the field. After this discontinuity all spins have negative magnetic energy. However inspection of the lowest energy configuration symmetries (App. D) does not reveal a pattern away from small and high fields that could predict the number of discontinuities for arbitrary N without doing the full calculation. In addition the calculation is numerically demanding for a complete detection of the jumps for $N > 180$, and as discussed before Fig. 2 shows that it is not straightforward to identify a simple origin of the discontinuities even for $N = 80$, both of which would also be helpful for a prediction of the number of gaps as a function of N .

The importance of the multiple discontinuities of the D_{5d} molecules is highlighted by comparing with the corresponding number for the slightly different D_{5h} molecules, shown in Figs. 3(c) and 3(d). Their number is fixed for all clusters (up to $N = 170$ was calculated), and the only change is that a low-field susceptibility gap becomes one of the magnetization for $N \geq 110$. Again they tend to approach constant values of $\frac{h}{h_{sat}}$ with N . In fact, the low-field magnetization discontinuity corresponds to the highest low-field magnetization jump of the D_{5d} molecules, and the high-field susceptibility gap to the high-field susceptibility discontinuity of the D_{5d} molecules. The strength of the magnetization discontinuity per spin is shown in Fig. 3(f), and equals $\Delta M = 0.764$ for $N = 170$. The different behavior of the D_{5d} and D_{5h} molecules shows the importance of subtle spatial symmetry differences for the magnetic response. Even though both resemble armchair nanotubes and only differ in symmetry by having a center of inversion (D_{5d}) instead of a plane of symmetry (D_{5h}), their magnetic response is quite different. Similar effects are known for the electronic structure properties of carbon nanotubes [8–11].

The importance of fullerene topology is further revealed with molecules that have the form of carbon nanotubes but are capped with six pentagons neighboring each other. Like the molecules capped with isolated pen-

tagons their number of vertices is a multiple of 10, and they have D_{5d} symmetry when it is an even and D_{5h} symmetry when it is an odd multiple of 10 [32]. The locations of the magnetization and susceptibility discontinuities and the corresponding change in the magnetization per spin are plotted in Fig. 4. In this case there is only one low-field magnetization and one high-field susceptibility discontinuity, whose locations with respect to $\frac{h}{h^{sat}}$ are practically constant already for relatively small N . In addition, spatial symmetry makes no difference in the magnetic response of these molecules.

In conclusion, it was shown that a class of fullerene molecules of D_{5d} spatial symmetry which have the shape of carbon nanotubes and are capped at the edges with

six-pentagon subblocks have a number of classical ground state magnetization discontinuities which increases with their size. This occurs when classical spins mounted at their vertices interact according to the AHM. The effect is sensitive to spatial symmetry as the D_{5h} molecules have a qualitatively different magnetic response. Richer magnetic behavior is expected when other frustrated fullerene molecules are encapsulated in the ones considered in this paper. The findings in this paper show that the specific topology of the molecules causes unexpected magnetic response in the classical AHM, and it is hoped that in the quantum case relaxing the limit of large on-site interaction U to more realistic values will also generate interesting magnetic behavior [46].

-
- [1] S. Iijima, *Nature (London)* **354**, 56 (1991).
 - [2] R. Saito, G. Dresselhaus, and M. S. Dresselhaus, *Physical Properties of Carbon Nanotubes* (Imperial College Press, London, 1998).
 - [3] C. Dekker, *Physics Today* **52**, 22 (1999).
 - [4] M. Terrones, *Annu. Rev. Mater. Res.* **33**, 419 (2003).
 - [5] M. F. L. D. Volder, S. H. Tawfik, R. H. Baughman, and A. J. Hart, *Science* **339**, 535 (2013).
 - [6] N. de Jonge, M. Doytcheva, M. Allieux, M. Kaiser, S. A. M. Mentink, K. B. K. Teo, R. G. Lacerda, and W. I. Milne, *Adv. Mater.* **17**, 451 (2005).
 - [7] B. Peng, M. Locascio, P. Zapol, S. Li, S. L. Mielke, G. C. Schatz, and H. D. Espinosa, *Nat. Nanotechnol.* **3**, 626 (2008).
 - [8] B. Q. Wei, R. Vajtai, and P. M. Ajayan, *Appl. Phys. Lett.* **79**, 1172 (2001).
 - [9] J. W. Mintmire, B. I. Dunlap, and C. T. White, *Phys. Rev. Lett.* **68**, 631 (1992).
 - [10] N. Hamada, S.-I. Sawada, and A. Oshiyama, *Phys. Rev. Lett.* **68**, 1579 (1992).
 - [11] R. Saito, M. Fujita, G. Dresselhaus, and M. S. Dresselhaus, *Appl. Phys. Lett.* **60**, 2204 (1992).
 - [12] E. Pop, D. Mann, Q. Wang, K. Goodson, and H. J. Dai, *Nano Lett.* **6**, 96 (2006).
 - [13] A. K. Geim and K. S. Novoselov, *Nat. Mater.* **6**, 183 (2007).
 - [14] A. H. C. Neto, F. Guinea, N. M. R. Peres, K. S. Novoselov, and A. K. Geim, *Rev. Mod. Phys.* **81**, 109 (2009).
 - [15] C. Kane, L. Balents, and M. P. A. Fisher, *Phys. Rev. Lett.* **79**, 5086 (1997).
 - [16] M. Bockrath, D. H. Cobden, J. Lu, A. G. Rinzler, L. B. R. E. Smalley, and P. L. McEuen, *Nature* **397**, 598 (1999).
 - [17] D. A. Siegel, W. Regan, A. V. Fedorov, A. Zettl, and A. Lanzara, *Phys. Rev. Lett.* **110**, 146802 (2013).
 - [18] F. Freitag, J. Trbovic, M. Weiss, and C. Schönenberger, *Phys. Rev. Lett.* **108**, 076602 (2012).
 - [19] S. Y. Zhou, D. A. Siegel, A. V. Fedorov, and A. Lanzara, *Phys. Rev. Lett.* **101**, 086402 (2008).
 - [20] A. S. Mayorov, D. C. Elias, M. Mucha-Kruczynski, R. V. Gorbachev, T. Tudorovskiy, A. Zhukov, S. V. Morozov, M. I. Katsnelson, V. I. Falko, A. K. Geim, et al., *Science* **333**, 860 (2011).
 - [21] T. Luu and T. A. Lähde, *cond-mat/1511.04918*.
 - [22] A. Auerbach, *Interacting Electrons and Quantum Magnetism* (Springer Verlag, New York, 1998).
 - [23] P. Fazekas, *Lecture Notes on Electron Correlation and Magnetism* (World Scientific, Singapore, 1999).
 - [24] W. Liang, M. Bockrath, D. Bozovic, J. H. Hafner, M. Tinkham, and H. Park, *Nature* **411**, 665 (2001).
 - [25] S. J. Tans, M. H. Devoret, H. Dai, A. Thess, R. E. Smalley, L. J. Geerligs, and C. Dekker, *Nature* **386**, 474 (1997).
 - [26] M. Bockrath, D. H. Cobden, P. L. McEuen, N. G. Chopra, A. Zettl, A. Thess, and R. E. Smalley, *Science* **275**, 1922 (1997).
 - [27] D. H. Cobden and J. Nygård, *Phys. Rev. Lett.* **89**, 046803 (2002).
 - [28] M. Hagiwara, M. Ikeda, T. Kida, K. Matsuda, S. Tadera, H. Kyakuno, K. Yanagi, Y. Maniwa, and K. Okunishi, *J. Phys. Soc. Jpn.* **83**, 113706 (2014).
 - [29] P. W. Anderson, *Mater. Res. Bull.* **8**, 153 (1973).
 - [30] H. T. Diep, *Frustrated Spin Systems* (World Scientific, Singapore, 2005).
 - [31] J. Schnack, *Dalton Trans.* **39**, 4677 (2010).
 - [32] P. W. Fowler and D. E. Manolopoulos, *An Atlas of Fullerenes* (Oxford University Press, Oxford, 1995).
 - [33] S. L. Altmann and P. Herzig, *Point-Group Theory Tables* (Oxford University Press, London, 1994).
 - [34] A. F. Hebard, M. J. Roseinsky, R. C. Haddon, D. W. Murphy, S. H. Glarum, T. T. M. Palstra, A. P. Ramirez, and A. R. Kortan, *Nature (London)* **350**, 600 (1991).
 - [35] S. Chakravarty, M. Gelfand, and S. Kivelson, *Science* **254**, 970 (1991).
 - [36] G. Stollhoff, *Phys. Rev. B* **44**, 10998 (1991).
 - [37] D. Coffey and S. A. Trugman, *Phys. Rev. Lett.* **69**, 176 (1992).
 - [38] N. P. Konstantinidis, *Phys. Rev. B* **72**, 064453 (2005).
 - [39] N. P. Konstantinidis, *Phys. Rev. B* **76**, 104434 (2007).
 - [40] N. P. Konstantinidis, *Phys. Rev. B* **80**, 134427 (2009).
 - [41] C. Schröder, H.-J. Schmidt, J. Schnack, and M. Luban, *Phys. Rev. Lett.* **94**, 207203 (2005).
 - [42] N. P. Konstantinidis, *J. Phys.: Condens. Matter* **27**, 076001 (2015).
 - [43] F. Lin, E. S. Sørensen, C. Kallin, and A. J. Berlinsky, *Phys. Rev. B* **75**, 075112 (2007).
 - [44] F. Lin and E. S. Sørensen, *Phys. Rev. B* **78**, 085435 (2008).

- (2008).
- [45] H. Yang, C. M. Beavers, Z. Wang, A. Jiang, Z. Liu, H. Jin, B. Mercado, M. M. Olmstead, and A. L. Balch, *Angew. Chem. Int. Ed.* **49**, 886 (2010).
 - [46] O. V. Yazyev, *Rep. Prog. Phys.* **73**, 056501 (2010).
 - [47] N. P. Konstantinidis, *Eur. Phys. J. B* **88**, 167 (2015).
 - [48] N. P. Konstantinidis, *J. Phys.: Condens. Matter* **28**, 016001 (2016).
 - [49] A. Machens, N. P. Konstantinidis, O. Waldmann, I. Schneider, and S. Eggert, *Phys. Rev. B* **87**, 144409 (2013).

Appendix A: Six Pentagon Subblocks

The subblock of six pentagons shown in Fig. 1(a) is the unit that causes frustration as part of a fullerene molecule. When the interpentagon coupling $J' = 0$ the magnetization curve corresponds to that of an isolated pentagon, which has constant susceptibility up to saturation with all spins sharing the polar angle in an umbrella configuration (Fig. 1(b)). For higher J' and low fields nearest-neighbor spins that belong to different pentagons remain very close to antiparallel, while nearest-neighbor intrapentagon correlations start to deviate from their isolated pentagon value. The central pentagon has the strongest exchange energy and the smallest net spin, as each of the other pentagons has two spins with only two nearest neighbors which are therefore freer to respond to the field. Right above the low-field magnetization discontinuity all polar angles become less than $\frac{\pi}{2}$, therefore each spin has negative magnetic energy. This is a spin umbrella configuration directly evolving from the $J' = 0$ configuration, however now the spins do not share a common polar angle. After the second magnetization discontinuity the configuration is the most symmetric. The inner ring spins, which belong to the central pentagon, share a common polar angle, their nearest neighbors that define another ring a different polar angle and so on for a total of four distinct polar angles, one for each ring. The pentagon in the middle has again the strongest exchange energy and the smallest net spin, while the other five pentagons have the same exchange energy and net spin. The introduction of the interpentagon coupling therefore generates two magnetization discontinuities which survive up to $J' = J$.

Appendix B: Zero Field Ground State Energy and Saturation Field

Nearest-neighbor spin directions in the zero-field ground state of an isolated pentagon have a relative angle of $\frac{4\pi}{5}$. For an isolated hexagon nearest-neighbors are antiparallel. If assembling pentagons and hexagons together to form a fullerene molecule with N vertices would not introduce further frustration, the ground state energy should be equal to the sum of the ground state energies of the isolated pentagons and hexagons, which

is $60\cos\frac{4\pi}{5} - (\frac{3N}{2} - 60)$. This is not the case for the fullerene molecules with D_{5d} and D_{5h} symmetry that are capped with two six-pentagon subblocks with isolated pentagons, with their energy being slightly higher (Fig. 5(a)). On the other hand, the $N = 60$ molecule has I_h symmetry and achieves the lowest possible energy. The ground state energy per site $\frac{E_{gr,h=0}}{N}$ approaches asymptotically with N the unfrustrated isolated hexagon value of $-\frac{3}{2}$. The only intrapentagon nearest-neighbor correlations equal to $\cos\frac{4\pi}{5}$ are the ones of the top and bottom pentagons (central pentagon in Fig. 1(a)). In addition, the spins of the top and bottom pentagon are antiparallel to their nearest-neighbors, which belong to different pentagons. The saturation field for the molecules is given in Table I and plotted in Fig. 5(b), and approaches asymptotically with N the value of 6.

Appendix C: Ground State Spin Configuration Changes at the Discontinuities

When the magnetic field is zero the spins of the top and bottom pentagon (central pentagon in Fig. 1(a)) are antiparallel to their nearest-neighbors that belong to different pentagons (App. B). Once the field becomes non-zero two pairs are left that maintain their antiparallel directions, with one of the spins of the pair lined up with the field, and the other antiparallel with it. This shows that for low fields the spins belonging to the pentagons respond differently as part of the molecule, in comparison with the isolated six pentagon subblock (App. A). When the field gets strong enough these pairs of spins cease to be antiparallel, and also parallel or antiparallel to the field. This change of their constant direction is accompanied by the low-field susceptibility discontinuity for $N \leq 140$, and by the lowest field magnetization discontinuity for $N = 160$ and 180 (Fig. 6). Similarly, in the ground state configuration just before saturation the spins at the top and bottom two levels of the molecules become aligned with the field (Fig. 7). This change to a constant direction occurs again with a discontinuity in the susceptibility.

The total magnetization S_i^z , $i = 1, \dots, \frac{N}{10} + 2$ for groups of spins that are at the same distance from the edges is the lowest for spins closer to the edges of the molecules for low fields (Fig. 6). $i = 1$ corresponds to the inner ring spins, which belong to the central pentagon (Fig. 1(a)), $i = 2$ to their nearest neighbors that define another ring and so on. In an open chain the individual spins respond to the field more strongly the closer to the edges they are [49]. Eventually the field makes the magnetization of these levels among the highest after the last of the low-field discontinuities, which is associated with the strongest change in magnetization in Fig. 3(e). Above this discontinuity all the spins have negative magnetic energy for the first time. The data for the magnetization and susceptibility discontinuities is given in Tables II and III.

TABLE I: Saturation magnetic field for the D_{5d} and D_{5h} fullerene molecules capped on both sides with six pentagons not neighboring each other. The columns give the number of vertices and the saturation magnetic field. The D_{5d} molecules have N equal to an even number times 10, while the D_{5h} molecules have N equal to an odd number times 10. The $N = 60$ molecule belongs to the I_h symmetry group [39].

N	h_{sat}
60	$\frac{9+\sqrt{5}}{2}$
70	5.73205
80	5.80194
90	5.84776
100	5.87939
110	5.90211
120	5.91899
130	5.93185
140	5.94188
150	5.94986
160	5.95630
170	5.96157
180	5.96595

Appendix D: Symmetry of the Ground State Spin Configurations

The symmetry of the lowest classical energy configuration of the D_{5d} fullerene molecules capped with two six-pentagon subblocks with isolated pentagons is determined from its nearest-neighbor correlations, with the requirement that a symmetry operation does not change their value between any two spins. The symmetry groups that leave the correlations unchanged are subgroups of D_{5d} [33] and are given in Table IV. The symmetry is highest for small fields and close to saturation. The zero field ground state spin configuration is unchanged for symmetry operations that belong to the S_{10} group. When the field becomes non-zero the symmetry is reduced to C_i . Right above the third discontinuity the only symmetry operation is the identity. The symmetry group right above the highest-field discontinuity is S_{10} , while right below it it is C_i . The wider column points to the symmetry of the configuration that is the lowest energy state for the widest range of fields. It occurs in the middle of the field range, and it is the first ground state configuration where all spins have negative magnetic energy.

TABLE II: Magnetization discontinuities for the D_{5d} fullerene molecules capped on both sides with six pentagons not neighboring each other. The columns give the number of vertices, the magnetic field for which the discontinuity occurs with respect to the saturation field, the magnetization right below the discontinuity with respect to the saturated magnetization, and the corresponding value for the magnetization right above the discontinuity. The $N = 60$ molecule belongs to the I_h symmetry group [39]. The data is plotted in Figs. 3(a), 3(b) and 3(e).

N	$\frac{h}{h_{sat}}$	$\frac{\hat{M}_-}{N}$	$\frac{\hat{M}_+}{N}$
60	0.14692	0.11723	0.14790
60	0.94165	0.94574	0.94651
80	0.13391	0.1153196	0.1369667
80	0.85562	0.87382668	0.87397773
80	0.92235	0.9411153	0.9412365
100	0.12544	0.1121451	0.1122307
100	0.13624	0.123827	0.133446
100	0.87742	0.89852222	0.89858053
100	0.91318	0.9343398	0.9343756
120	0.13508	0.125082	0.125743
120	0.13958	0.13803	0.14309
120	0.88966	0.91044946	0.91046701
120	0.91169	0.9322856	0.9322932
140	0.12906	0.1204307	0.1205064
140	0.14067	0.136563	0.143995
140	0.81364	0.83215130	0.83215559
140	0.89669	0.9162739	0.9162788
140	0.91305	0.93230792	0.93230936
160	0.10540	0.0984430	0.0984548
160	0.12282	0.1153954	0.1154144
160	0.13977	0.134215	0.134328
160	0.14146	0.139161	0.144565
160	0.86579	0.8838119	0.8838135
160	0.90128	0.9194573	0.9194584
160	0.91522	0.9330304	0.9330306
180	0.091760	0.08618793	0.08619039
180	0.11857	0.1121242	0.1121302
180	0.13624	0.1302571	0.1302697
180	0.14180	0.14047	0.14469
180	0.88446	0.90136320	0.90136369
180	0.90536	0.92215730	0.92215752
180	0.91719	0.93365306	0.93365312

TABLE III: Susceptibility discontinuities for the D_{5d} fullerene molecules capped on both sides with six pentagons not neighboring each other. The columns give the number of vertices, and the magnetic field for which the discontinuity occurs with respect to the saturation field. The data is plotted in Figs. 3(a) and 3(b).

N	$\frac{h}{h_{sat}}$
80	0.1187
80	0.9546
100	0.1179
100	0.1364
100	0.9400
120	0.1121
120	0.9333
140	0.1078
140	0.9296
160	0.9273
180	0.9258

TABLE IV: Symmetry of the ground state spin configurations. The first symmetry column refers to the case of zero field. The field increases when going to the right.

N	lowest energy configuration symmetry									
80	S_{10}	C_i	C_i	I	I			C_i	S_{10}	
100	S_{10}	C_i	C_i	I	I	I		I	C_i	S_{10}
120	S_{10}	C_i	I	I	I			I	C_i	S_{10}
140	S_{10}	C_i	I	I	C_i		I	I	C_i	S_{10}
160	S_{10}	C_i	I	I	C_i	C_i	I	I	C_i	S_{10}
180	S_{10}	C_i	I	I	C_i	C_i	I	I	C_i	S_{10}

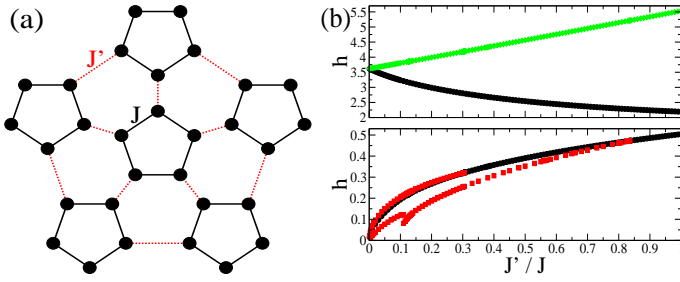


FIG. 1: (Color online) (a) Planar projection of the six-pentagon subblock that is the source of frustration for the D_{5d} and D_{5h} fullerene molecules resembling carbon nanotubes. The circles are classical spins of unit magnitude and each one interacts with its nearest neighbors according to the connecting lines. The (black) solid and (red) dashed lines indicate intrapentagon interactions of strength J and interpentagon interactions of strength J' respectively. J' varies from 0 to J . (b) The (black) filled circles show the magnetization discontinuities, while the (red) filled squares the susceptibility discontinuities as functions of $\frac{J'}{J}$ and the magnetic field h . The (green) diamonds show the saturation field.

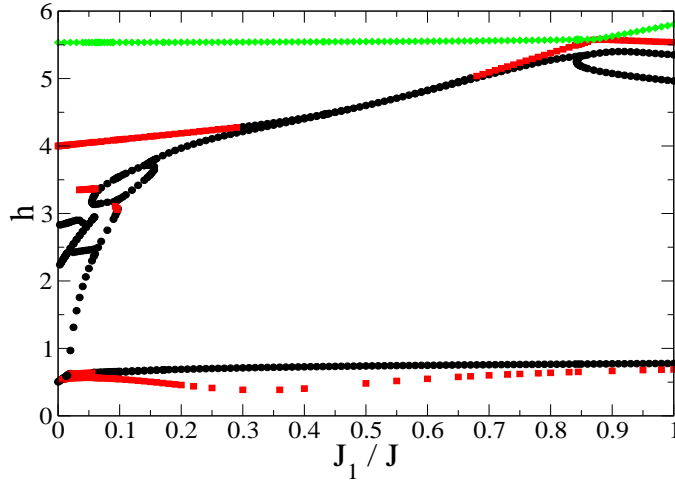


FIG. 2: (Color online) Evolution of the discontinuities for the D_{5d} molecule with $N = 80$ as a function of the relative coupling $\frac{J_1}{J}$ between the two six-pentagon subblocks at the edges and the spins that form the nanotube, and the magnetic field h . The (black) filled circles show the magnetization discontinuities, while the (red) filled squares the susceptibility discontinuities. The (green) diamonds show the saturation field.

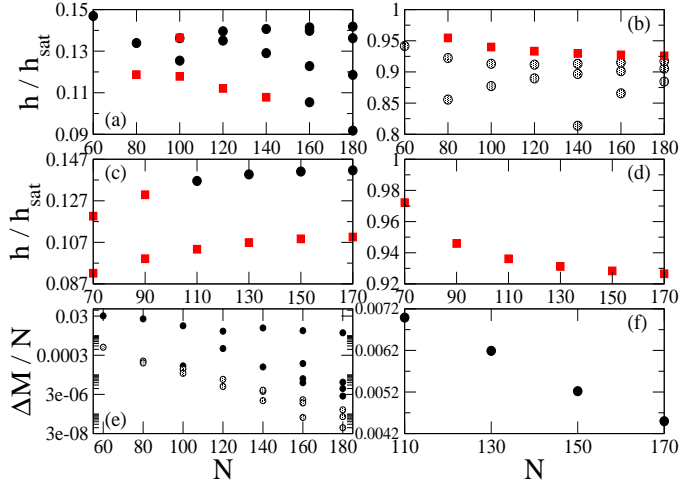


FIG. 3: (Color online) (a), (b) Magnetization and susceptibility discontinuities for the D_{5d} molecules which have the shape of carbon nanotubes and are capped on both sides with six pentagons that are not neighboring each other. They are given as functions of the number of vertices N and the reduced magnetic field $\frac{h}{h_{sat}}$, with h_{sat} the saturation magnetic field ($N = 60$ corresponds to the I_h symmetry molecule [39]). The (black) filled circles and the (black) dotted circles show respectively the low- and high-field magnetization discontinuities, while the (red) filled squares the susceptibility discontinuities. (c), (d) Similarly for the D_{5h} molecules. (e), (f) Corresponding strengths of the magnetization discontinuities ΔM per spin for the D_{5d} and D_{5h} molecules respectively.

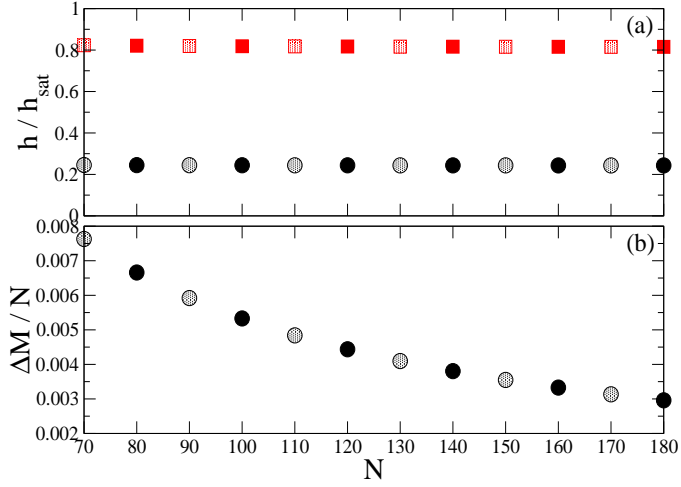


FIG. 4: (Color online) (a) Magnetization and susceptibility discontinuities for the D_{5d} and D_{5h} molecules which have the shape of carbon nanotubes and are capped on both sides with six pentagons that are neighboring each other. They are given as functions of the number of vertices N and the reduced magnetic field $\frac{h}{h_{sat}}$, with h_{sat} the saturation magnetic field. The (black) filled and the (black) dotted circles show respectively the magnetization discontinuities for the D_{5d} and D_{5h} molecules, while the (red) filled and the (red) dotted squares the corresponding susceptibility discontinuities. (b) Corresponding strengths of the magnetization discontinuities ΔM per spin.

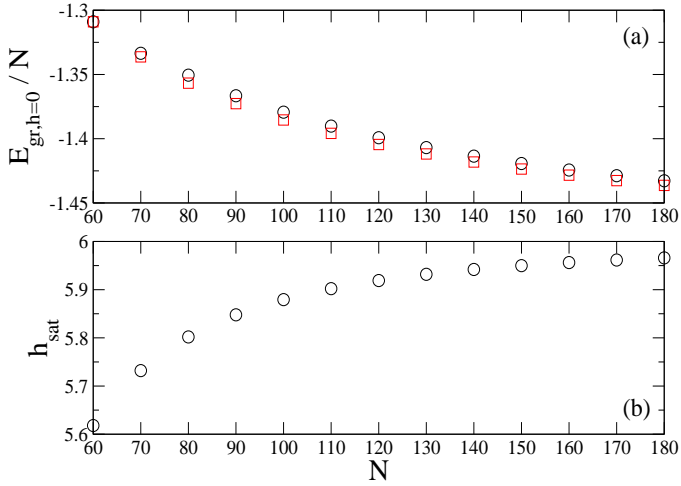


FIG. 5: (a) (Color online) The (black) circles show the zero field lowest energy per spin $\frac{E_{gr,h=0}}{N}$ as a function of the number of vertices N for the fullerene molecules with D_{5d} and D_{5h} symmetry that are capped with the two six-pentagon subblocks with isolated pentagons. The (red) squares show the sum of the energies of the corresponding isolated pentagons and hexagons per spin. $N = 60$ corresponds to the I_h symmetry molecule [39]. (b) Saturation field as a function of N .

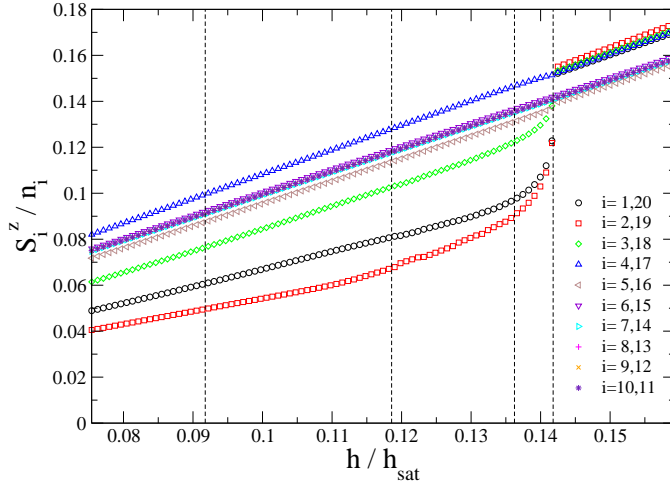


FIG. 6: (a) (Color online) The different symbols (and colors) show the total magnetization per spin $\frac{S_i^z}{n_i}$ for each level of the spins according to their distance from one of the edges, given as a function of the magnetic field over its saturation value $\frac{h}{h_{sat}}$ for the $N = 180$ cluster. The number of spins per level n_i equals 5 for $i = 1, 2, 19, 20$, and 10 for any other i . The dashed lines show the fields for the magnetization discontinuities. The values are symmetric with respect to the central plane of the cluster.

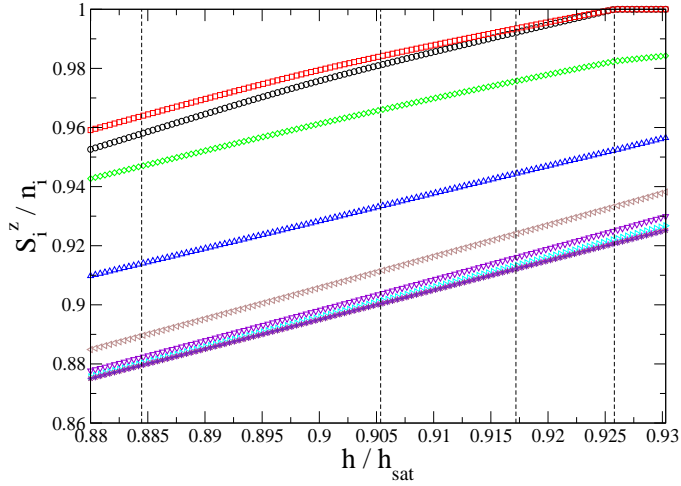


FIG. 7: (a) (Color online) Total magnetization per spin $\frac{S_i^z}{n_i}$ for each level of the spins according to their distance from one of the edges, given as a function of the magnetic field over its saturation value $\frac{h}{h_{sat}}$ for the $N = 180$ cluster. The different symbols (and colors) follow Fig. 6. The number of spins per level n_i equals 5 for $i = 1, 2, 19, 20$, and 10 for any other i . The dashed lines show the fields for the magnetization discontinuities. The values are symmetric with respect to the central plane of the cluster.